among the prime candidates to harbor proton-translocation sites, distances for energy-transfer reactions of more than 100 Å have to be envisaged. A continuous electron density most likely corresponding to an α helix is laterally associated with the membrane arm embedded in the transmembrane segments near the matrix-facing surface (Fig. 3). With a length of 60 Å oriented in parallel to the long axis of the membrane arm, it extends from the end of the proximal domain about half-way into the distal domain (Fig. 2A). At the proximal end, it is connected by continuous electron density to one of the transmembrane segments in a nearly orthogonal orientation. Strikingly, on the P_D domain side, it terminates close to electron density features resembling a discontinuous helix arrangement, suggesting the presence of a proton-translocation unit (Fig. 3B) (*22*). We propose that this observed connection between the P domains is a critical transmission element within the proton-pumping machinery of complex I.

The modular architecture of complex I as revealed by crystallographic analysis of the complete mitochondrial enzyme is summarized in Fig. 4. In a bipartite functional organization, conformational energy is generated by the redox chemistry occurring in the N and Q modules of the peripheral arm and is transmitted to the two proton-pumping modules of the membrane arm, which are connected by a helical transmission element.

References and Notes

1. U. Brandt, *Annu. Rev. Biochem.* **75**, 69 (2006).
2. M. K. F. Wikström, *FEBS Lett.* **169**, 300 (1984).
3. A. Galkin, S. Dröse, U. Brandt, *Biochim. Biophys. Acta* **1757**, 1575 (2006).
4. A. Galkin, U. Brandt, *J. Biol. Chem.* **280**, 30129 (2005).
5. L. Kussmaul, J. Hirst, *Proc. Natl. Acad. Sci. U.S.A.* **103**, 7607 (2006).
6. M. T. Lin, M. F. Beal, *Nature* **443**, 787 (2006).
7. V. Rhein *et al.*, *Proc. Natl. Acad. Sci. U.S.A.* **106**, 20057 (2009).
8. H. Fukui, C. T. Moraes, *Trends Neurosci.* **31**, 251 (2008).
9. M. Radermacher *et al.*, *J. Struct. Biol.* **154**, 269 (2006).
10. T. Clason *et al.*, *J. Struct. Biol.* **169**, 81 (2010).
11. L. A. Sazanov, P. Hinchliffe, *Science* **311**, 1430 (2006).
12. J. M. Berrisford, L. A. Sazanov, *J. Biol. Chem.* **284**, 29773 (2009).
13. M. L. Verkhovskaya, N. Belevich, L. Euro, M. Wikström, M. I. Verkhovsky, *Proc. Natl. Acad. Sci. U.S.A.* **105**, 3763 (2008).
14. D. Esterhazy, M. S. King, G. Yakovlev, J. Hirst, *Biochem.* **47**, 3964 (2008).
15. P. Hinchliffe, L. A. Sazanov, *Science* **309**, 771 (2005).
16. V. Zickermann *et al.*, *Biochim. Biophys. Acta* **1787**, 574 (2009).
17. C. Mathiesen, C. Hägerhäll, *Biochim. Biophys. Acta* **1556**, 121 (2002).
18. S. Kerscher, S. Dröse , K. Zwicker, V. Zickermann, U. Brandt, *Biochim. Biophys. Acta* **1555**, 83 (2002).
19. N. Morgner *et al.*, *Biochim. Biophys. Acta* **1777**, 1384 (2008).
20. A. Abdrakhmanova *et al.*, *Biochim. Biophys. Acta* **1658**, 148 (2004).
21. Materials and methods are available as supporting material on *Science* Online.
22. E. Screpanti, C. Hunte, *J. Struct. Biol.* **159**, 261 (2007).
23. D. J. Morgan, L. A. Sazanov, *Biochim. Biophys. Acta* **1777**, 711 (2008).
24. E. A. Baranova, D. J. Morgan, L. A. Sazanov, *J. Struct. Biol.* **159**, 238 (2007).
25. G. Belevich, L. Euro, M. Wikstrom, M. Verkhovskaya, *Biochem.* **46**, 526 (2007).
26. K. Zwicker *et al.*, *J. Biol. Chem.* **281**, 23013 (2006).
27. M. A. Tocilescu, U. Fendel, K. Zwicker, S. Kerscher, U. Brandt, *J. Biol. Chem.* **282**, 29514 (2007).
28. U. Fendel, M. A. Tocilescu, S. Kerscher, U. Brandt, *Biochim. Biophys. Acta* **1777**, 660 (2008).
29. M. A. Tocilescu *et al.*, *Biochim. Biophys. Acta* **1797**, 625 (2010).
30. V. Zickermann *et al.*, *J. Biol. Chem.* **278**, 29072 (2003).
31. T. Clason, V. Zickermann, T. Ruiz, U. Brandt, M. Radermacher, *J. Struct. Biol.* **159**, 433 (2007).
32. T. Friedrich, *J. Bioenerg. Biomembr.* **33**, 169 (2001).

33. Excellent technical assistance by K. Siegmund and technical support by A. Duchene, F. Streb, and B. Wenzel are gratefully acknowledged. We thank S. Kerscher for his essential contributions regarding all aspects of *Y. lipolytica* genetics and B. Wrzesniewska for testing the impact of antibody fragments to improve crystallization. We are indebted to H. Michel for valuable advice during the initial stages of the project and for his continuous support. We thank the European Synchrotron Radiation Facility and the Swiss Light Source (SLS) for granting beam time, many scientists especially at SLS beamlines X06SA and X10SA for constantly supporting our work, and the staff of the Helmholtz Zentrum für Infektionsforschung (HZI)/Gesellschaft für Biotechnologische Forschung, Braunschweig for large-scale fermentation of *Y. lipolytica*. Funding by the Deutsche Forschungsgemeinschaft (SFB 472 Projects P2 and P17) is gratefully acknowledged. This study was supported by the Excellence Initiative of the German Federal and State Governments (EXC 115 and EXC 294). Electron density maps are available on request.

Supporting Online Material

www.sciencemag.org/cgi/content/full/science.1191046/DC1
Materials and Methods
Fig. S1
Tables S1 and S2
References

16 April 2010; accepted 10 June 2010
Published online 1 July 2010;
10.1126/science.1191046
Include this information when citing this paper.

An Electronic Bus Bar Lies in the Core of Cytochrome bc_1

Monika Świerczek,[1] Ewelina Cieluch,[1] Marcin Sarewicz,[1] Arkadiusz Borek,[1] Christopher C. Moser,[2] P. Leslie Dutton,[2] Artur Osyczka[1]*

The ubiquinol–cytochrome c oxidoreductases, central to cellular respiration and photosynthesis, are homodimers. High symmetry has frustrated resolution of whether cross-dimer interactions are functionally important. This has resulted in a proliferation of contradictory models. Here, we duplicated and fused cytochrome b subunits, and then broke symmetry by introducing independent mutations into each monomer. Electrons moved freely within and between monomers, crossing an electron-transfer bridge between two hemes in the core of the dimer. This revealed an H-shaped electron-transfer system that distributes electrons between four quinone oxidation-reduction terminals at the corners of the dimer within the millisecond time scale of enzymatic turnover. Free and unregulated distribution of electrons acts like a molecular-scale bus bar, a design often exploited in electronics.

Figure 1 shows a bacterial ubiquinol–cytochrome c oxidoreductase (*1*), often called cytochrome bc_1, displaying homodimeric core subunit structure typical of respiratory and photosynthetic electron transfer systems (*2*, *3*). It is well established that adjacent cofactors in each monomer serve to separate electronic charge across the membrane in the catalytically relevant microsecond-to-millisecond electron transfer process (*4*, *5*). However, high structural, spectroscopic, and electrochemical symmetry between the monomers of the dimer has confounded efforts to determine whether a functional electron-transfer connection exists between monomers. At the distances displayed in Fig. 1, calculations show that electron-tunneling times between cofactors in different monomers are much slower than the physiologically relevant time scale, except for tunneling between the two b_L hemes. Electron tunneling across the 13.9 Å separating these two hemes is calculated to be in the 0.025- to 0.25-ms range (*5*), slightly faster than the measured 0.5- to 5.0-ms physiological turnover time. However, electron-tunneling theory itself (*6*, *7*) provides only an upper limit for the rate of electron transfer between redox cofactors. Many electron transfers in oxidoreductases are limited not by electron tunneling but by slower coupled events of chemistry, conformational change, or motion (*8*, *9*). Indeed, many models have been proposed for ubiquinol–cytochrome c oxidoreductases that include just such regulation of electron transfer within or between monomers (*10*–*15*) or even strict electronic isolation of monomers (*16*). Given the inherent tunneling speed, a relatively small amount of coupling of this electron tunneling to chemical or conformational events could effectively regulate interaction between monomers or even isolate them (*10*–*16*).

To resolve the underlying dimer engineering, we broke the symmetry of the cytochrome bc_1 homodimer from *Rhodobacter capsulatus* shown

[1]Department of Biophysics, Faculty of Biochemistry, Biophysics and Biotechnology, Jagiellonian University, Kraków, Poland. [2]The Johnson Research Foundation, Department of Biochemistry and Biophysics, University of Pennsylvania, PA 19104, USA.

*To whom correspondence should be addressed. E-mail: artur.osyczka@uj.edu.pl

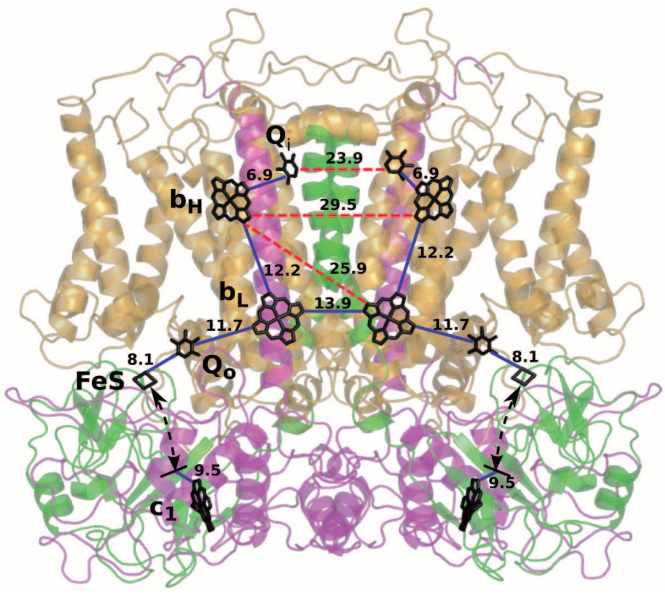

Fig. 1. Cofactors and distances in homodimer of cytochrome bc_1 [Protein Data Bank ID: 1ZRT (*1*)]. Each monomer comprises cytochrome b (yellow), cytochrome c_1 (magenta), and FeS subunit (green). Functional distances (blue lines) and nonfunctional distances (red dashed lines) between cofactors (black) are in angstroms. Q_o site quinone is approximated from the crystallographic position of stigmatellin (*1*), and Q_i site quinone position is adopted from (*28*). FeS head domain movement (*29*) is indicated by the dashed arrow.

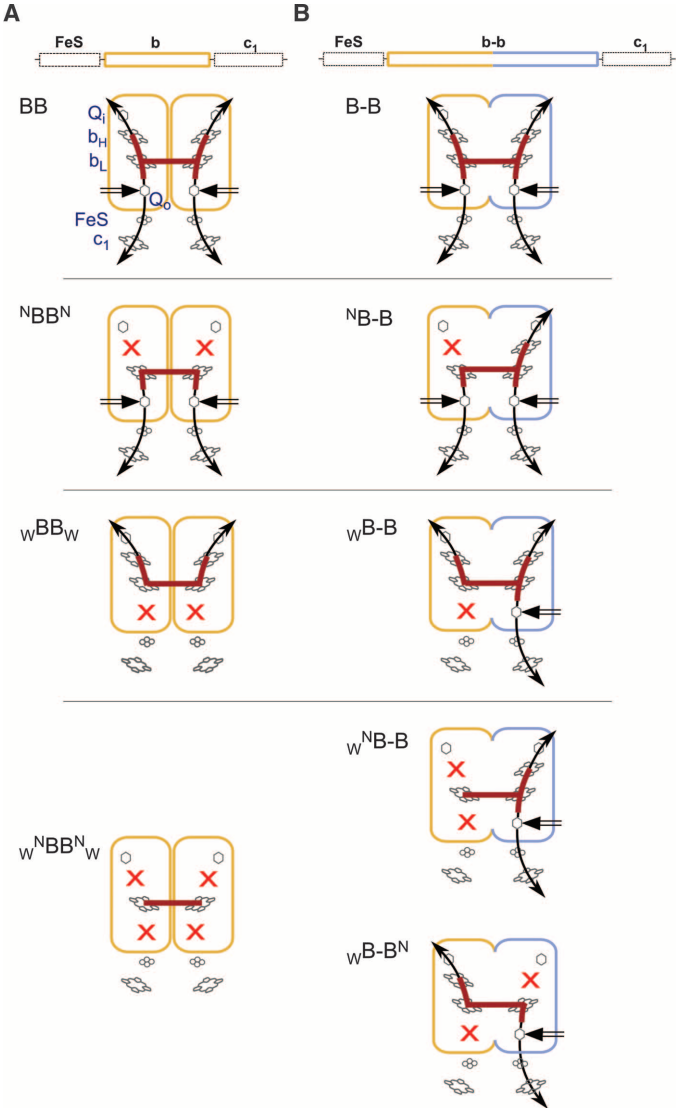

Fig. 2. Symmetric and asymmetric knockout patterns. Distribution of the knockouts (red crosses) constructed with unfused native operon coding (**A**) and fused gene coding (**B**). BB, native dimer: $^{N}BB^{N}$, both upper branches removed; $_{W}BB_{W}$, both lower branches removed; $_{W}{}^{N}BB^{N}{}_{W}$, all four branches removed. B-B, fused protein: ^{N}B-B, one upper branch removed; $_{W}$B-B, one lower branch removed; $_{W}{}^{N}$B-B, two branches on the same side removed; $_{W}$B-B^{N}, two branches across removed. N and W refer to H212N and G158W point mutations in cytochrome b (G, Gly; H, His; N, Asn; W, Trp). Black arrows, functional branches. Black double arrow, electron entry point at the Q_o site. Brown overlay: intraprotein electronic bus bar.

in Fig. 1. We genetically fused two identical monomeric cytochrome b subunits, analogous to the successful fusion of two membrane-anchored cytochromes c in *R. capsulatus* (*17*). The cytochrome b subunits accommodate the core cofactors in the electron-transfer chain and the putative bridge between monomers (Figs. 1 and 2). The N and C termini of the eight-transmembrane–α-helical chain of the monomeric cytochrome b protrude at the cytoplasmic side of the membrane. We joined these termini by extending the gene encoding cytochrome b with the linker peptide sequence followed by the second copy of the same gene containing Strep-tag at its C terminus (figs. S2 and S3) (*18*). The other two genes of the operon, encoding the subunits containing the FeS cluster and heme c_1, were left unchanged. Wild-type and fused cytochrome bc_1 are designated BB and B-B, respectively. Electrophoresis verified that the subunits of B-B had the correct molecular mass (fig. S4), and ultraviolet (UV)–visible and electron paramagnetic resonance spectroscopy (EPR) demonstrated normal cofactor assembly (Fig. 3 and figs. S5 and S6). Measurements of electron transfer in B-B (see below) indicated that the fused protein remained functional.

To uncover dimer-specific operation and test the putative H-shaped electron transfer system, we need only two asymmetrically positioned point mutations in B-B. We chose two sites that have been extensively characterized in BB. The mutation H212N (symmetrical $^{N}BB^{N}$ in Fig. 2A) prevents heme b_H assembly without affecting other cofactors in the cytochrome bc_1 structure (*5*). This heme b_H knockout markedly cuts short electron transfer in both upper H branches and, because upper and lower branches are energetically coupled, diminishes quinol oxidation levels at the Q_o site and linked electron transfer into the lower branch. The second site, G158W (symmetrical $_{W}BB_{W}$ in Fig. 2A), prevents substrate quinol binding at the Q_o site (Q_o site knockout), again without affecting the function of the other cofactors, and effectively inactivates dual electron transfer from quinol into both lower and upper branches (*4*). We achieved expression and assembly of mutants with asymmetrically placed copies of H212N or G158W in B-B, either separately or together in various combinations [table S1 and supporting online material (SOM) text]. Figure S4 confirms the proper size of the subunits of B-B in these asymmetric single- and double-mutant forms, and Fig. 3 and figs. S5 and S6 demonstrate that levels of expressed heme b_H (reported by UV-visible spectra) or occupied Q_o site (reported by the EPR spectrum of the FeS cluster) are precisely half that of the native cytochrome bc_1, as expected.

As depicted in Fig. 2B, permutations of these two strategically positioned mutations unambiguously expose all possible electron-transfer paths through the individual branches and bridge of this H-shaped electron transfer system. Figure 4 shows two types of kinetic assays, flash-induced on the left and steady-state on the right. After a flash of light activates the photosynthetic reaction

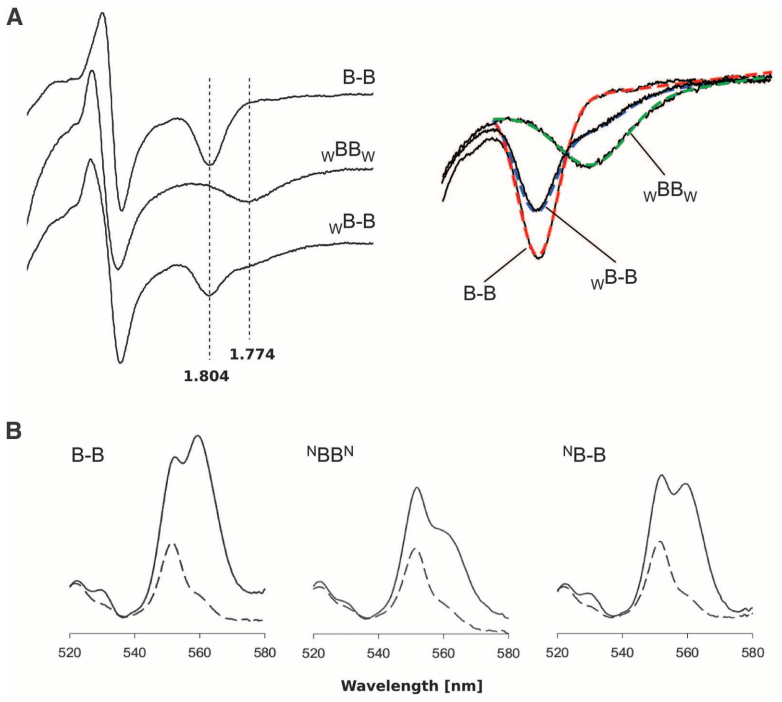

Fig. 3. Spectroscopic proof of structural asymmetry imposed by mutations in B-B. (**A**) X-band continuous-wave EPR spectra of the FeS cluster in membranes. Left: B-B with native g_x transition at 1.804 (intact Q_o site); $_wBB_W$ with g_x broadened and shifted to 1.774 (disabled Q_o site); $_wB$-B shows two distinct g_x transitions of 1.804 and 1.774. Right: g_x in $_wB$-B fitted with linear combinations of two Gaussian curves (blue) obtained from fitting of single Gaussian curve to the shape of g_x in B-B (red) and $_wBB_W$ (green) with equal contribution of each component. To produce such spectra, mutated and nonmutated Q_o sites in $_wB$-B must each communicate with one head domain of the FeS subunit, as expected for an assembly of one fusion protein per set of two FeS subunits. (**B**) Optical redox difference spectra of hemes in membranes: B-B with native-like spectrum with hemes C (peak at 550 nm) and B (peak at 560 nm) components; $^NBB^N$ with diminished amplitude at 560 nm reflecting absence of both hemes b_H in dimer; ^{N}B-B shows decreased peak at 560 nm with the amplitude in between that of the spectrum of B-B and $^NBB^N$, as expected for a loss of only one heme b_H in ^{N}B-B. Solid and dashed lines, dithionite minus ferricyanide and ascorbate minus ferricyanide spectra, respectively.

Table 1. Enzymatic activity supported by the complete H-shaped electron transfer system and its truncated derivatives.

Name*	Turnover rate† (1/s)	
	Without inhibitor	With antimycin‡
BB	56.4	3.2
$^NBB^N$	1.6	1.7
$_wBB_W$	0.1	0.1
B-B	60.0	3.4
^{N}B-B	48.7	3.2
$_w$B-B (B-B_W)	51.9 (53.6)	2.0 (2.1)
$_w{}^N$B-B (B-$B^N{}_W$)	36.4 (46.0)	1.9 (2.0)
$_w$B-B^N	26.1	1.3

*Letter code corresponds to schemes of Fig. 2. Obtainable second versions of some forms (table S1) and their activities are shown in parentheses. †Measured for cytochrome bc_1 in membranes. ‡Myxothiazol or stigmatellin in place of antimycin abolished activity to almost zero in all forms.

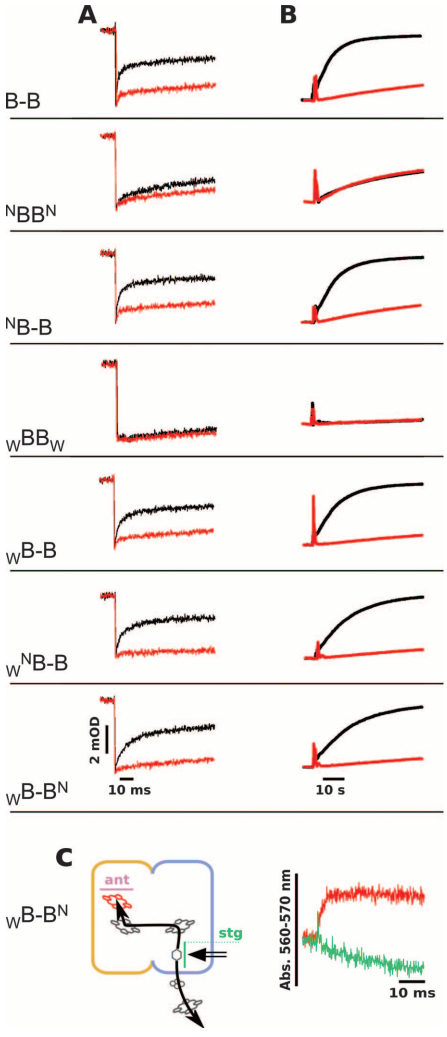

Fig. 4. Testing functional branch connection in the H-shaped electron transfer system. (**A**) Light-induced oxidation and re-reduction of cytochrome c at 550 minus 540 nm in membranes containing complete knockout variations described in Fig. 2. Black, uninhibited; red, inhibited with antimycin. B-B_W and B-$B^N{}_W$ displayed kinetics similar to that of $_wB$-B and $_w{}^NB$-B, respectively (not shown). (**B**) Corresponding steady-state enzymatic reduction of cytochrome c at 550 nm. Rates are listed in Table 1. (**C**) Light-induced heme b_H kinetics in $_wB$-B^N in the presence of antimycin abolishing Q_i action (red) or stigmatellin abolishing Q_o action (green). In $_wB$-B^N blocked with antimycin (ant), the only route to reduce heme b_H (red) must involve the heme b_L to b_L electron transfer. stg, stigmatellin.

center to oxidize cytochrome c, the re-reduction of cytochrome c provides a sensitive indicator of electron-transfer activity and quinol oxidation catalysis in cytochrome bc_1. Cytochrome c oxidation-reduction in B-B (Fig. 4A, top trace) is similar to that of wild-type BB (not shown). Flash-activated microsecond oxidation of cytochrome c is shown as a prompt downward change. In the ensuing milliseconds, the upward trending cytochrome c trace shows re-reduction by electrons coming through the lower branches of the H from oxidations of quinol in the Q_o site (Fig. 4A, top trace, black).

The critical involvement of upper and lower branches in quinol oxidation is demonstrated by inhibition by antimycin. It inactivates both Q_i sites and prevents movement of electrons through and out of the upper branches, which in turn restricts movement of electrons through and out of the lower branch to cytochrome c; thus cytochrome c reduction is greatly impeded (Fig. 4A, top trace, red). Similarly, the double, symmetric heme b_H knockout ($^NBB^N$) trims the upper branch at the point before the Q_i site and impedes cytochrome c reduction, even without antimycin (Fig. 4A, second trace). However, unlike the symmetric $^NBB^N$, the single asymmetric heme b_H knockout (^{N}B-B) that inactivates one of the two upper branches has cytochrome c re-reduction kinetics very similar to that of the knockout-free B-B (Fig. 4A, third trace). Parallel results are

found for the Q_o site mutants. Cytochrome c re-reduction in the double, symmetrical Q_o site knockout ($_WBB_W$) is impeded (Fig. 4A, fourth trace), whereas the inactivation of only one of the two lower branches (either $_WB$-B or B-B_W) reveals cytochrome c re-reduction kinetics only slightly slower than in knockout-free B-B (Fig. 4A, fifth trace). Moreover, knocking out both upper and lower branches of electron transfer in the same monomer ($_W{}^NB$-B or B-$B^N{}_W$) causes a similar minor slowing of cytochrome c re-reduction (Fig. 4A, second from bottom). These results demonstrate that the activity of one intact monomer is independent of the functional status of the other monomer.

The mutant combination $_WB$-B^N (Fig. 2B and Fig. 4A, bottom) allows investigation of cross monomer electron transfer. The result is unambiguous. After light-flash–induced oxidation of cytochrome c, re-reduction follows the same general pattern observed with the unmutated B-B and mutants with singly or doubly knocked out cofactors in the same chain of one monomer. Thus, flash-activated electron transfer occurs between the monomers on the millisecond time scale.

Figure 4B and Table 1 repeat these analyses with a dark, steady-state activity assay that is standard for cytochrome bc_1 in respiratory systems. These analyses confirm the results from flash activation in showing that for ^NB-B, $_WB$-B or B-B_W, $_W{}^NB$-B or B-$B^N{}_W$, and $_WB$-B^N the observed steady-state rates are never less than half that of B-B.

Figure 4C reveals approximately millisecond electron transfer across the bridge in $_WB$-B^N more directly by following heme b_H reduction. This roughly matches enzymatic turnover and demonstrates that intermonomer electron transfer is a physiologically relevant event. This time is also within the uncertainty of the calculated pure tunneling time, showing that any chemical or conformational events coupled to electron tunneling between hemes b_L must be minor, and is inconsistent with the view that electron transfer between the hemes b_L does not occur (*16*). Moreover, because inactivation of either monomer or any upper or lower monomer branch has no notable effect on the milliseconds or seconds time scale electron transfer throughout the dimer, there is serious doubt that intermonomer or interbranch conformational interactions play an important role in regulating energy coupling or function of cytochrome bc_1 (*10*–*15*).

In the absence of intricate regulation, the natural engineering of electron transfer connections in dimeric cytochrome bc_1 appears relatively simple and robust. Dimerization of proteins is common and proceeds for any number of different reasons. But merely by permitting two of the core redox cofactors on either side of a dimer interface to approach to within a 14 Å electron-tunneling distance, independent elementary redox chains are converted to an H-shaped electron transfer system that enables any connection between terminals on opposite sides of the membrane to be enzymatically competent. This simple electronic distribution to the four terminals of the dimer can be likened to a molecular version of a conducting bus bar familiar in electronics (fig. S1). The uniting action of the bus bar offers several advantages for respiration and photosynthesis, especially under stress. Multiple unpaired electrons produced at the Q_o site (*19*, *20*) and implicated in the production of reactive oxygen species (ROS) (*21*–*24*) can be collected and neutralized (*5*, *25*). The bus bar also builds in redundancy to allow physiological function of the protein even after operational damage of one part, perhaps from ROS. Finally, this design increases the effective diffusion target size for substrates ubiquinone and cytochrome c (*26*) that may be critical in the overcrowded bioenergetic membrane (*27*).

References and Notes

1. E. A. Berry *et al.*, *Photosynth. Res.* **81**, 251 (2004).
2. E. A. Berry, M. Guergova-Kuras, L. S. Huang, A. R. Crofts, *Annu. Rev. Biochem.* **69**, 1005 (2000).
3. W. A. Cramer, H. Zhang, J. Yan, G. Kurisu, J. L. Smith, *Annu. Rev. Biochem.* **75**, 769 (2006).
4. H. Ding *et al.*, *Biochemistry* **34**, 15979 (1995).
5. A. Osyczka, C. C. Moser, F. Daldal, P. L. Dutton, *Nature* **427**, 607 (2004).
6. C. C. Moser, J. M. Keske, K. Warncke, R. S. Farid, P. L. Dutton, *Nature* **355**, 796 (1992).
7. C. C. Page, C. C. Moser, X. Chen, P. L. Dutton, *Nature* **402**, 47 (1999).
8. C. C. Moser, S. E. Chobot, C. C. Page, P. L. Dutton, *Biochim. Biophys. Acta* **1777**, 1032 (2008).
9. C. C. Moser, C. C. Page, P. L. Dutton, *Phil. Trans. R. Soc. B* **361**, 1295 (2006).
10. O. A. Gopta, B. A. Feniouk, W. Junge, A. Y. Mulkidjanian, *FEBS Lett.* **431**, 291 (1998).
11. A. Y. Mulkidjanian, *Photochem. Photobiol. Sci.* **6**, 19 (2007).
12. R. Covian, B. L. Trumpower, *Biochim. Biophys. Acta* **1777**, 1079 (2008).
13. C. A. Yu *et al.*, *Biochim. Biophys. Acta* **1777**, 1038 (2008).
14. J. W. Cooley, D.-W. Lee, F. Daldal, *Biochemistry* **48**, 1888 (2009).
15. M. Castellani *et al.*, *J. Biol. Chem.* **285**, 502 (2010).
16. A. R. Crofts *et al.*, *Biochim. Biophys. Acta* **1777**, 1001 (2008).
17. D.-W. Lee, Y. Oztürk, A. Osyczka, J. W. Cooley, F. Daldal, *J. Biol. Chem.* **283**, 13973 (2008).
18. Materials and methods are available as supporting material on *Science* Online.
19. J. L. Cape, M. K. Bowman, D. M. Kramer, *Proc. Natl. Acad. Sci. U.S.A.* **104**, 7887 (2007).
20. H. Zhang, A. Osyczka, P. L. Dutton, C. C. Moser, *Biochim. Biophys. Acta* **1767**, 883 (2007).
21. M. Ksenzenko, A. A. Konstantinov, G. B. Khomutov, A. N. Tikhonov, E. K. Ruuge, *FEBS Lett.* **155**, 19 (1983).
22. F. Muller, A. R. Crofts, D. M. Kramer, *Biochemistry* **41**, 7866 (2002).
23. S. Dröse, U. Brandt, *J. Biol. Chem.* **283**, 21649 (2008).
24. A. Borek, M. Sarewicz, A. Osyczka, *Biochemistry* **47**, 12365 (2008).
25. V. P. Shinkarev, C. A. Wraight, *FEBS Lett.* **581**, 1535 (2007).
26. M. Sarewicz, A. Borek, F. Daldal, W. Froncisz, A. Osyczka, *J. Biol. Chem.* **283**, 24826 (2008).
27. R. J. Ellis, *Trends Biochem. Sci.* **26**, 597 (2001).
28. C. Hunte, J. Koepke, C. Lange, T. Rossmanith, H. Michel, *Structure* **8**, 669 (2000).
29. E. Darrouzet, C. C. Moser, P. L. Dutton, F. Daldal, *Trends Biochem. Sci.* **26**, 445 (2001).

30. We are grateful to F. Daldal (University of Pennsylvania, Philadelphia, USA) for the genetic system for cytochrome bc_1 in *R. capsulatus*. This work was supported by The Wellcome Trust International Senior Research Fellowship (A.O.) and by the United States National Institutes of Health (P.L.D.)

Supporting Online Material

www.sciencemag.org/cgi/content/full/329/5990/451/DC1
Materials and Methods
SOM Text
Figs. S1 to S6
Table S1
References

14 April 2010; accepted 9 June 2010
10.1126/science.1190899

Sfrp5 Is an Anti-Inflammatory Adipokine That Modulates Metabolic Dysfunction in Obesity

Noriyuki Ouchi,[1]* Akiko Higuchi,[1] Koji Ohashi,[1] Yuichi Oshima,[1] Noyan Gokce,[2] Rei Shibata,[3] Yuichi Akasaki,[1] Akihiko Shimono,[4] Kenneth Walsh[1]*

Adipose tissue secretes proteins referred to as adipokines, many of which promote inflammation and disrupt glucose homeostasis. Here we show that secreted frizzled-related protein 5 (Sfrp5), a protein previously linked to the Wnt signaling pathway, is an anti-inflammatory adipokine whose expression is perturbed in models of obesity and type 2 diabetes. Sfrp5-deficient mice fed a high-calorie diet developed severe glucose intolerance and hepatic steatosis, and their adipose tissue showed an accumulation of activated macrophages that was associated with activation of the c-Jun N-terminal kinase signaling pathway. Adenovirus-mediated delivery of Sfrp5 to mouse models of obesity ameliorated glucose intolerance and hepatic steatosis. Thus, in the setting of obesity, Sfrp5 secretion by adipocytes exerts salutary effects on metabolic dysfunction by controlling inflammatory cells within adipose tissue.

Obesity is a predisposing factor for metabolic disorders, such as type 2 diabetes, which are often associated with a low-grade inflammatory state in adipose tissue. Adipose tissue secretes a variety of cytokines, referred to as adipokines (*1*–*3*). Most adipokines—such as tumor necrosis factor α (TNFα), interleukin-6 (IL-6), and leptin—are proinflammatory. One prominent exception is adiponectin (APN), an anti-inflammatory adipokine that promotes insulin sensitization and protects cardiovascular tissue from ischemic injury (*2*, *4*).

Because adipokine dysregulation can contribute to the pathogenesis of obesity-linked disorders, we sought to identify new adipokines by comparing the gene expression profile of adipose tissue

Science

An Electronic Bus Bar Lies in the Core of Cytochrome bc_1

Monika Swierczek, Ewelina Cieluch, Marcin Sarewicz, Arkadiusz Borek, Christopher C. Moser, P. Leslie Dutton and Artur Osyczka

Science **329** (5990), 451-454.
DOI: 10.1126/science.1190899

Heme Communication Revealed by Asymmetry

An electronic bus bar is an electrical conductor that connects several circuits. **Swierczek *et al.*** (p. 451) now find that a similar strategy is used by the protein cytochrome bc_1 that plays a central role in cellular respiration and photosynthesis. Protein engineering was used to break the symmetry of a cytochrome bc_1 homodimer, which revealed that the dimer is bridged by electron transfer between two hemes. This allows electrons to move freely within and between dimers to distribute between four catalytic sites.